SUPPLEMENTAL MATERIAL

Neuroinflammation plays a critical role in cerebral cavernous malformation disease

Catherine Chinhchu Lai[1*], Bliss Nelsen[1*], Eduardo Frias-Anaya[1*], Helios Gallego-Gutierrez[1*], Marco Orecchioni[2], Victoria Herrera[1], Elan Ortiz[1], Hao Sun[1], Omar A. Mesarwi[1], Klaus Ley[2], Brendan Gongol[3,4,&], Miguel Alejandro Lopez-Ramirez[1,5,&]

[1]Department of Medicine, University of California, San Diego, La Jolla, California, USA. [2]Division of Inflammation Biology, La Jolla Institute for Immunology, La Jolla, California, USA. [3] Department of Health Sciences, Victor Valley College, Victorville, California, USA. [4]Institute for Integrative Genome Biology, 1207F Genomics Building, University of California, Riverside, CA 92521, USA. [5]Department of Pharmacology, University of California, San Diego, La Jolla, California, USA.

[*]These authors contributed equally

[&]These senior authors contributed equally

Running title: Neuroinflammation in CCM disease

Address correspondence to:

Dr. Brendan Gongol and Miguel A. Lopez-Ramirez

Victor Valley college, Victorville, CA, 92395, &

9500 Gilman Diver, BSB 5096, La Jolla, CA 92093

Telephone: 858-534-4425, FAX: 858-822-6458

Brendan.gongol@ucr.edu

malopezramirez@health.ucsd.edu

Conflict of interest statement: The authors have declared that no conflict of interest exists

Online Supplemental Materials
Expanded Material & Methods
Data supplement figures S1 to S9
Data supplement statistical tables I-IV
Reference 62

Expanded Materials and Methods (Online Supplement)

Material and methods

Genetically modified animals

Brain endothelial-specific conditional *Pdcd10*-null mice were generated by crossing a *Slco1c1* promoter-driven tamoxifen-regulated Cre recombinase (*Slco1c1-CreERT2,* a gift from Markus Schwaninger, University of Lübeck) strain with loxP-flanked *Pdcd10* (*Pdcd10*$^{fl/fl}$, a gift from Wang Min, Yale University;*Slco1c1-CreERT2;Pdcd10*$^{fl/fl}$) mice. Brain endothelial-specific conditional *Ikkb*-null mice were generated by *Slco1c1-CreERT2* strain with loxP-flanked *IKKb* (*Ikkb*$^{fl/fl}$, a gift from Michael Karin, UCSD;*Slco1c1-CreERT2;Ikkb*$^{fl/fl}$). On a postnatal day 1 (P1), mice were administered 50 µg of 4-hydroxy-tamoxifen (H7904, Sigma-Aldrich) by intragastric injection to induce genetic inactivation of the endothelial *Pdcd10* gene in littermates with *Slco1c1-CreERT2;Pdcd10*$^{fl/fl}$ (*Pdcd10*^{BECKO}), and *Pdcd10*$^{fl/fl}$ mice were used as littermate controls. Injection of 4-hydroxy-tamoxifen at P5 was also performed and led to reduced CCM burden[10] and was used to assess lesions when the brain endothelial *Ikkb* gene was inactivated. We also used non-injected *Slco1c1-CreERT2;Pdcd10*$^{fl/fl}$ mice as littermate controls whose gene expression and histology were the same as in *Pdcd10*$^{fl/fl}$ mice. To perform Translational Ribosome Affinity Purification (TRAP) in astrocytes[18] we generated *Slco1c1-iCreERT2;Pdcd10*$^{fl/fl}$*;Aldh1l1-EGFP/Rpl10a* and controls littermate *Pdcd10*$^{fl/fl}$*;Aldh1l1-EGFP/Rpl10a.* All animal experiments were performed in compliance with animal procedure protocols approved by the University of California, San Diego Institutional Animal Care and Use Committee.

Astrocyte ribosome isolation

Aldh1l1-EGFP/Rpl10a mice crossed with the CCM mouse model were used to isolate TRAP mRNAs from astrocytes using the protocol and instructions as previously described[13]. Astrocyte-TRAP mRNAs were from brains of mice age P75.

Brain endothelial cell (BEC) isolation

Adult P75 *Pdcd10*$^{BECKO;}$*Aldh1l1-EGFP/Rpl10a* mice (*Pdcd10*^{BECKO}) and *Pdcd10*$^{fl/fl}$;*Aldh1l1-EGFP/Rpl10a* (*Pdcd10*$^{fl/fl}$) control littermates were sacrificed, and their brains were isolated and placed into cold solution A (0.5% bovine serum albumin (BSA) in DMEM and 1 µg/µl glucose, 10mM HEPES, 1x penicillin-streptomycin). Meninges and choroid plexus were removed, and one brain of *Pdcd10*^{BECKO} mice was minced using scissors in cold solution A. We used two brains of *Pdcd10*$^{fl/fl}$ mice that were pooled together to collect enough microvasculatures. Brain tissue suspension was then centrifuged at 1000g for 5 minutes at 4°C. The supernatant was removed and the tissue was digested with a collagenase/dispase solution (1mg/ml collagenase/dispase [Sigma-Aldrich], 20 units/ml DNase I [Sigma-Aldrich], and 0.150µg/ml tosyl-lysine-chloromethyl-ketone [Sigma-Aldrich] in DMEM])(51) at 37°C for 1 hour with vigorous shaking every 10 minutes. Tissue suspension was triturated using thin-tipped Pasteur pipettes until fully homogenous and centrifuged at 700g for 5 minutes at 4°C. The supernatant was removed, and the pellet was resuspended in 20ml of 25% BSA solution followed by centrifugation at 1000g for 20 minutes at 4°C. Capillary fragments were pulled down to the bottom of the tube, remaining BSA and myelin were discarded, and the pellet was resuspended in cold solution A followed by centrifugation at 700g for 5 minutes at 4°C. The supernatant was removed, and capillary fragments were incubated in collagenase/dispase solution at 37°C for 1 hour. Solution A was added to inactivate enzymatic activity, and the suspension was centrifuged once at 700g for 5 minutes at 4°C. The cell pellet was resuspended in ACK lysis (Gibco) buffer to lyse red blood cells, and then cells were centrifuged once at 700g for 5 minutes at 4°C. The supernatant was removed, and cells were then incubated with anti-CD45 coated beads and passed through a column, following the manufacturer's protocol (Miltenyi Biotec). Isolated BECs were recovered by negative selection and used for RNA-seq and histology analysis.

Leukocyte isolation and flow cytometry analysis

Pdcd10^{BECKO} mice and *Pdcd10*$^{fl/fl}$ control littermates were sacrificed, brains were collected and placed into cold solution A. Meninges, brain stem, white matter/brainstem were removed. Brain tissue was triturated using scissors and centrifuged at 1000g for 5 minutes. The supernatant was removed, and the pellet was incubated in pre-warmed collagenase/dispase solution for 40 minutes at 37°C (with vigorous shaking every 10 minutes). After incubation, cold solution A was used to stop enzymatic activity, and the suspension was centrifuged at 600g for 10 minutes at 4°C. The supernatant was removed, and the cell pellet was resuspended into a Percoll gradient (70% Percoll, 37% Red Percoll, 30% Percoll, respectively) as previously described by Guldner et

al., followed by centrifugation at 1000g for 25 minutes at room temperature. The final solution consisted of three distinct layers, with a buffy leukocyte layer at the interface of clear 70% Percoll and 37% Red Percoll and a thick myelin layer at the top of the tube. The leukocyte layer was extracted and resuspended in cold 1X HBSS in a fresh tube, followed by centrifugation at 600g for 7 minutes at 4°C. The supernatant was removed, and cells were resuspended in flow cytometry buffer (0.5% BSA, 2mM EDTA in PBS1X).

Flow cytometry characterization of immune cells

After isolation cells were stained in the dark for 30 min at 4C with a mixture of anti-mouse CD45-PerCP (clone 30-F11, Biolegend), CD11b-PE-Cy7 (clone M1/70, Biolegend), TCRβ- PE (clone H57-597, Biolegend), CD4-BV786 (clone GK1.5, Invitrogen), CD8-BV421 (clone 53-6.7, Biolegend). CD19-APC-Cy7 (clone 6D5, Biolegend), Ly6G-FITC (clone 1A8, BD Biosciences), F4/80-BV711 (clone BM8, Biolegend), CD206-BV650 (clone C068C2, Biolegend), Ly6C-PE (clone HK1.4, Biolegend), CD64-APC (clone X54-5/7.1, Biolegend), CD11c-BV570 (clone N418, Biolegend), and CX3CR1-BV510 (clone SA011F11, Biolegend) antibodies and the LD FVS700 fixable dye (cat# 564997, BD Biosciences). After staining, cells were washed with 1 mL of flow cytometry buffer, and fixed in 1x IC fixation buffer (e-biosciences) for 20 min at RT in the dark. Fixed cells were washed and resuspended in flow cytometry buffer, and acquired on a LSRII flow cytometer (BD Biosciences). Unstained cells and FMOs samples were also acquired as controls. Data was acquired with the FACSDiva software (BD Biosciences) and analyzed with FlowJo software (Treestar Inc).

RNA isolation

Total RNA from brain tissue and BECs were isolated by TRIzol method according to the manufacturer's instructions (Thermo Fisher Scientific). For brains tissue and cells, 1ml of TRIzol was used to homogenize the tissue by passing it through a syringe several times. The lysates were transferred to Phase Lock Gel 2ml tubes, and 200μl of chloroform (Thermo Fisher Scientific) was added to each tube, mixing vigorously for 15 seconds, followed by incubation at room temperature for 3 minutes. Samples were then centrifuged at 12000g for 10 minutes at 4°C, and the aqueous phases containing RNA were collected and transferred to 1.5ml DNAse/RNAse free microfuge tubes. To precipitate RNA, 500μl of isopropanol was added, samples were resuspended and incubated for 10 minutes at room temperature followed by centrifugation at 12000g for 10 minutes at 4°C. The supernatant was removed, and the pellet was washed with

1ml of 75% ethanol followed by centrifugation at 7500g for 5 minutes at 4°C. RNA was resuspended in water and the quantity (ND-1000 spectrophotometer; NanoDrop Technologies) and quality (TapeStation; Agilent) of total RNA were analyzed. Detailed procedures and complete RNAseq data are available in the U.S. National Center for Biotechnology Information (Bethesda, MD, USA) Gene Expression Omnibus (GEO) under accession number GSE204979 (http://www.ncbi.nlm.nih.gov/geo).

RT-qPCR analysis

A total RNA amount of 300 ng was used to produce single-stranded complementary DNA (cDNA) using random primers according to the manufacturer's protocol (Thermo Fisher Scientific). For gene expression analysis, 10 ng of cDNA was used with the Kapa SybrFast qPCR master mix (Kapa Biosystems) and thermal cycler (CFX96 Real-Time System; Bio-Rad) were used to determine the relative levels of the genes analyzed according to the manufacturer's protocol. Actin mRNA levels were used as internal control, and the $2^{-\Delta\Delta CT}$ method was used for analyses of the data.

RNA-sequencing (RNA-seq)

Total RNA was assessed for quality using an Agilent Tapestation 4200, and 50 nanograms of RNA from samples with an RNA Integrity Number (RIN) greater than 8.0 were used to generate RNA-seq libraries using the Illumina® Stranded mRNA Prep (Illumina, San Diego, CA). Samples were processed following manufacturer's instructions. Resulting libraries were multiplexed and sequenced with 100 basepair (bp) Paired End reads (PE100) to a depth of approximately 25 million reads per sample on an Illumina NovaSeq 6000. Samples were demultiplexed using bcl2fastq Conversion Software (Illumina, San Diego, CA). Sequencing analysis was performed using the R programming environment and the RiboSeq systemPipeR workflow. All reads were aligned to the Mus Musculus GRCm39 genome version 104 using hisat2 read alignment software. Read counting was performed using the GenomicFeatures library and the corresponding GRCm39 GTF file from ensemble. All fold change calculations were performed using EdgeR. When values are normalized by a percentile ranking, the reads per kilobase per million (RPKM) values in the heatmap were normalized as previously described using the empirical cumulative distribution function in R to calculate the percent of values that have an equal or lesser value to each represented record[62]. This normalization was applied uniformly throughout the illustrated

data in order to provide an accurate representation of the magnitude of the values in relation to each other.

Inflammasome activity assay

BECs were isolated and resuspended in EBM-2 media (Lonza) supplemented with 0.1% gentamicin, 0.1% ascorbic acid, 0.1% heparin, and 0.2% BSA. Cells were incubated with the NLRP3 inhibitor MCC950 Sodium (10 μM;) or vehicle and seeded onto poly-lysine-treated coverslips for 1 hour at 37^{o}C. After incubation, coverslips were washed three times using 1X HBSS + Ca^{+2}, and then incubated with 30X FAM-FLICA Caspase-1 probe (ImmunoChemistry Technologies) in EBM-2 media plus supplements for 1 hour at 37^{o}C as described by the manufacturer's protocol (ImmunoChemistry Technologies). Rat monoclonal antibody against VCAM1 (Alexa-674 labelled, clone 429(MVCAM.A)) and CD45 (Alexa-594, clone S18009D) were incubated at room temperature for 30 min (BioLegend). Preparations were fixed in 4% PFA in PBS and mounted on microscope slides using Fluoromount-G mounting medium (SouthernBiotech). The slides were viewed with a fluorescent microscope (Keyence), and the images were captured with BZX-700 software (Keyence). The quantification analysis was performed using ImageJ Ver.1.53f on high-resolution images.

Immunohistochemistry

Brains from *Pdcd10*^{BECKO} and littermate control *Pdcd10*$^{fl/fl}$ mice at the specific age points were isolated and fixed in 4% PFA in PBS at 4^{o}C overnight. Tissue was placed into cryoprotective 30% sucrose solution in PBS, and then embedded and frozen in O.C.T compound (Fischer Scientific). Brains were cut using a cryostat into 18-μm sagittal sections onto Superfrost Plus slides (VWE International). Sections were incubated in a blocking-permeabilization solution (0.5% Triton X-100, 5% goat serum, 0.5% BSA, in PBS) for 2 hours and then incubated in rabbit polyclonal antibodies against GFAP (1:300; GA524; Agilent Dako), rat polyclonal antibodies against GFAP (1:200; Thermo Fisher Scientific), rabbit polyclonal antibodies against Iba1 (1:100; 019-19741; FUJIFILM Wako) in PBS at room temperature overnight. Slides were washed one time in brain Pblec buffer (1X PBS, 1mM CaCl2, 1mM MgCl2, 0.1 mM MnCl2, and 0.1% Triton X-100) and incubated with isolectin B4 (IB4) FITC conjugated (1:80, L2895; Sigma-Aldrich) in brain-Pblec buffer at 4^{o}C overnight. Tissue sections were washed four times in PBS and incubated with suitable Alexa Fluor coupled secondary antibodies (1:300, Thermo Fisher Scientific) in PBS for 2h at RT. Cell nuclei were stained with DAPI and mounted using Fluoromount-G mounting

medium (SouthernBiotech). Fresh frozen brain tissue was used to perform immunofluorescence analysis of leukocyte infiltration. Rat monoclonal antibody against CD41 (Alexa-488/594, clone MWReg30), CD45 (Alexa-fluor 594, clone S18009D), CX3CR1 (Alexa-fluor 488, clone SA011F11), LY6G (Alexa-fluor 488, clone 1A8), CD16/32 (PE/Dazzle 594, clone S17011E), CD206 (Alexa-fluor 488, clone C068C2), were incubated at room temperature for 30 min (BioLegend). Preparations were fixed in 4% PFA in PBS and incubated with rabbit polyclonal antibodies against GFAP overnight followed by isolectin B4 (IB4) biotin conjugated (1:80) in brain-Pblec buffer at 4°C overnight. After streptavidin (Alexa-Fluor 647) staining and followed by incubation with suitable Alexa Fluor coupled secondary antibodies, and the cell nuclei were stained with DAPI and mounted with Fluoromount-G mounting medium (SouthernBiotech). The slides were viewed with a high-resolution slide scanner (Olympus VS200 Slide Scanner), and the images were captured with VS200 ASW V3.3 software (Olympus). Quantifications were performed blinded. The quantification analysis was performed using ImageJ Ver. 1.53f on high-resolution images. Four to five brain sections per mouse were used for analysis.

CCM lesion quantification

Brains from *Pdcd10*^{BECKO}*Ikkb*$^{+/+}$, *Pdcd10*^{BECKO};*Ikkb*$^{BECKO/+}$ and *Pdcd10*^{BECKO};*Ikkb*^{BECKO} mice were isolated and fixed in 4% PFA at 4°C overnight. After cryoprotection, sucrose (30%) and freezing, 18 μm sections of sagittal brain tissue were cut onto Superfrost Plus slides (VWR International), and stained by the hematoxylin and eosin (5 brain sections/mouse, sections were performed from superior sagittal sinus to the cerebral hemisphere). Slides were imaged using NanoZoomer Slide Scanner (Hamamatsu Photonics; San Diego, USA). Lesions were analyzed as stage 1, single cavernous, or stage 2, multi-cavernous and thrombosis. Quantifications were performed blinded. The quantification analysis was performed using Hamamatsu Photonics software.

Statistical analysis

Statistical analysis was performed using Prism software (GraphPad). Data are expressed as mean values $\pm$ standard error of the mean (SEM) for multiple individual and biological experiments. For all experiments, the number of independent and biological replicates (n) is indicated. The Shapiro-Wilk normality test with alpha=0.05 assessed the normality of data. For comparison between two groups, Student's unpaired two-tail *t-test* or analysis of variance (ANOVA) for comparison among multiple groups, followed by the Tukey post hoc test, was used for normally distributed data. Mann-Whitney two-tailed test was used for two groups, and the

Kruskal-Wallis test, followed by Dunn's post hoc test, was used for non-normally distributed data. Sample sizes were calculated by assuming a two-sided alpha=0.05, 80% power, and homogeneous variances for two samples with the means and standard deviation from previous studies[4,13,15,16]. At least three biologically independent experiments were conducted to ensure reproducibility. No statistical across-test comparisons were performed in this manuscript.

Representative figures

Representative images were selected as the best representative image from a group of images taken in each experiment.

Supplemental Figure 1. Increase of hypoxia and coagulation signaling pathways in CCM

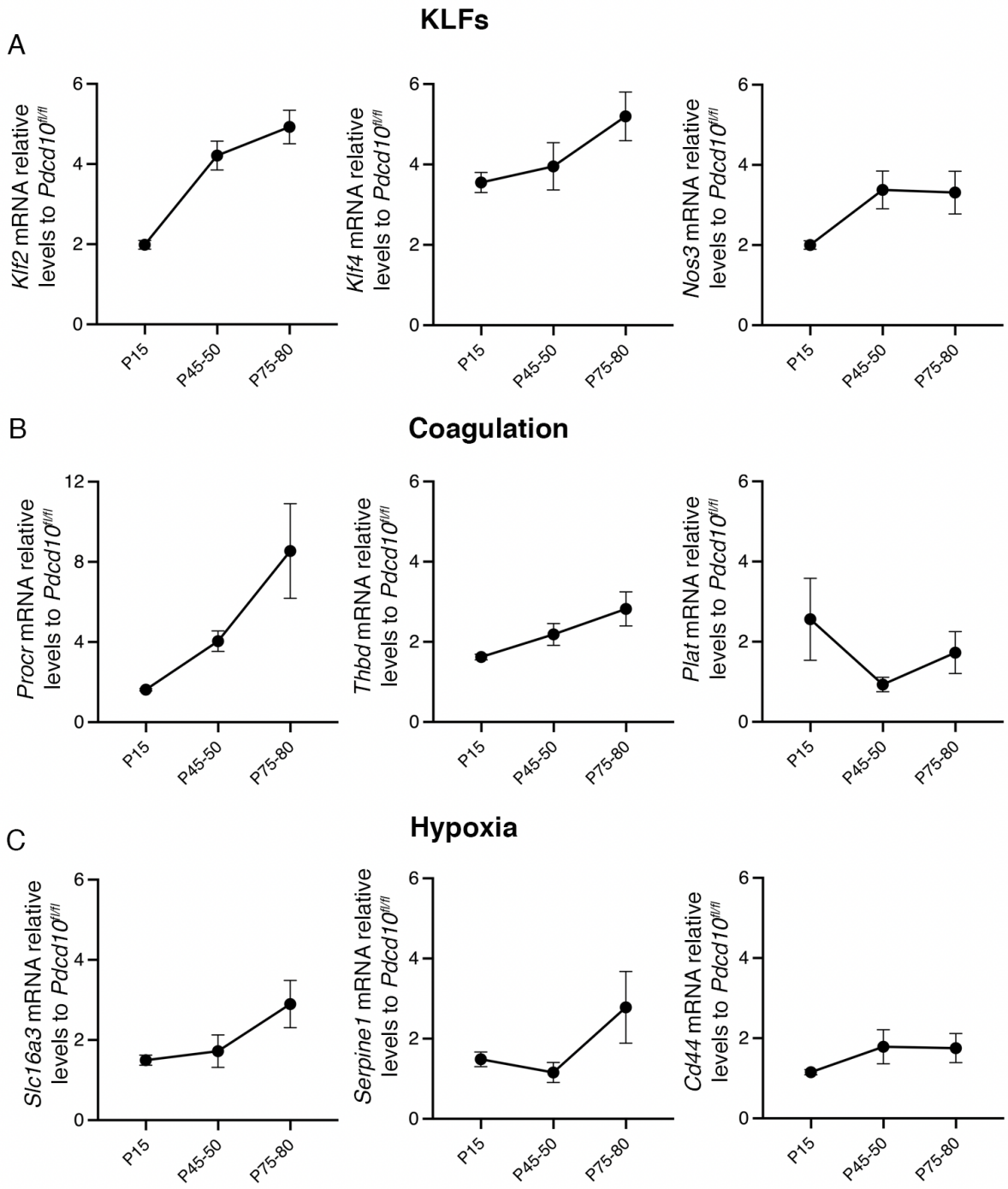

disease. CCM lesions are present in the cerebrum of *Pdcd10*^{BECKO} mice at acute (P15), progression (P50), and chronic stage (P80). **A,** Analysis of *Klf2*, *Klf4*, *Nos3*, **B,** Analysis of *Procr*, *Thbd*, *Plat*, **C,** Analysis of *Slc16a3, Serpine1,* and *Cd44* mRNA levels by RT-qPCR in cerebral tissue from mice in samples from Fig 1b. Cerebral tissue from *Pdcd10*$^{fl/fl}$ littermates were used as control. Data are mean ±SEM, P50 mice, n = 3; P15 and P80 mice n = 6.

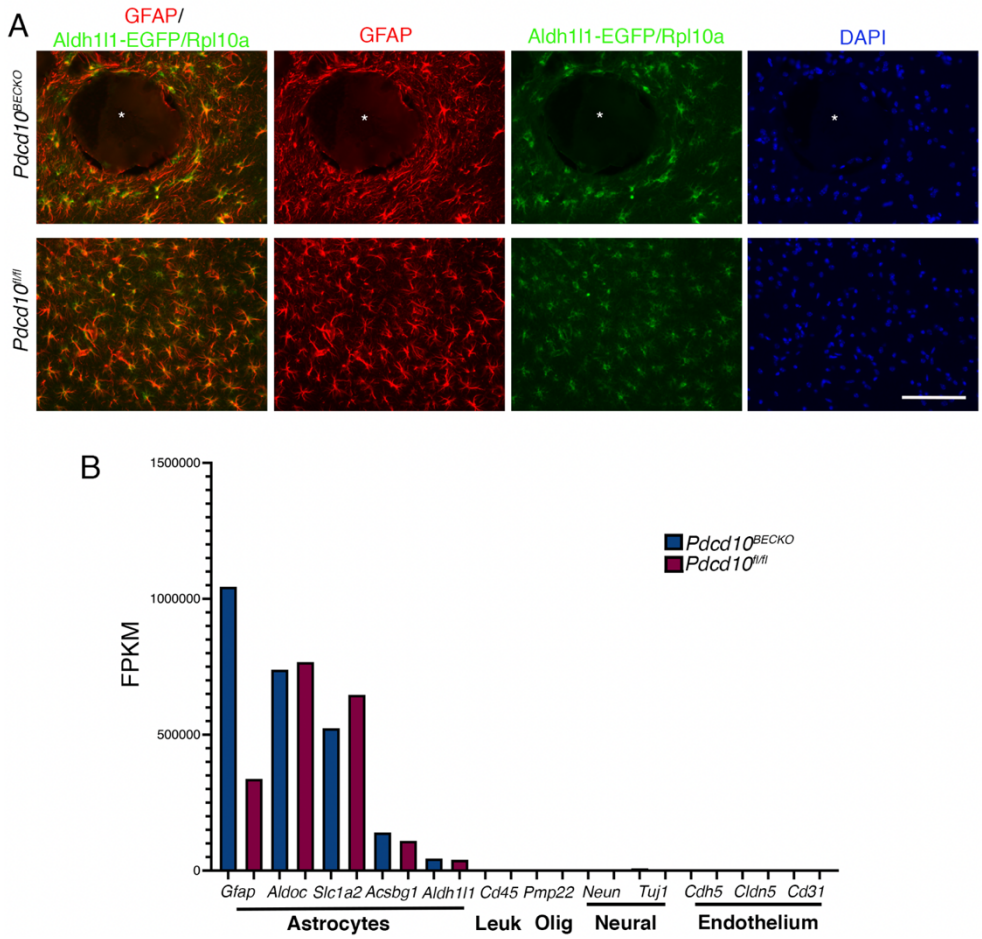

Supplemental Figure 2. Neuroinflammatory astrocytes in CCM disease. A, Immunofluorescence analysis show colocalization of GFAP+ astrocytes with cells expressing EGFP-RpL10a in *Pdcd10$^{fl/fl}$;Aldh1l1-EGFP/Rpl10a* brains sections. Asterisks denote the vascular lumen of CCM lesions. Scale bar is 100 μm. n = 3 mice in each group. **B,** Analysis of known brain cell-specific gene markers from *Pdcd10^{BECKO};Aldh1l1-EGFP/Rpl10a* (blue bar) and *Pdcd10$^{fl/fl}$;Aldh1l1-EGFP/Rpl10a* littermate controls (red bar) following ribosome-bound mRNA analysis by RNA-seq. n = 3 in each group.

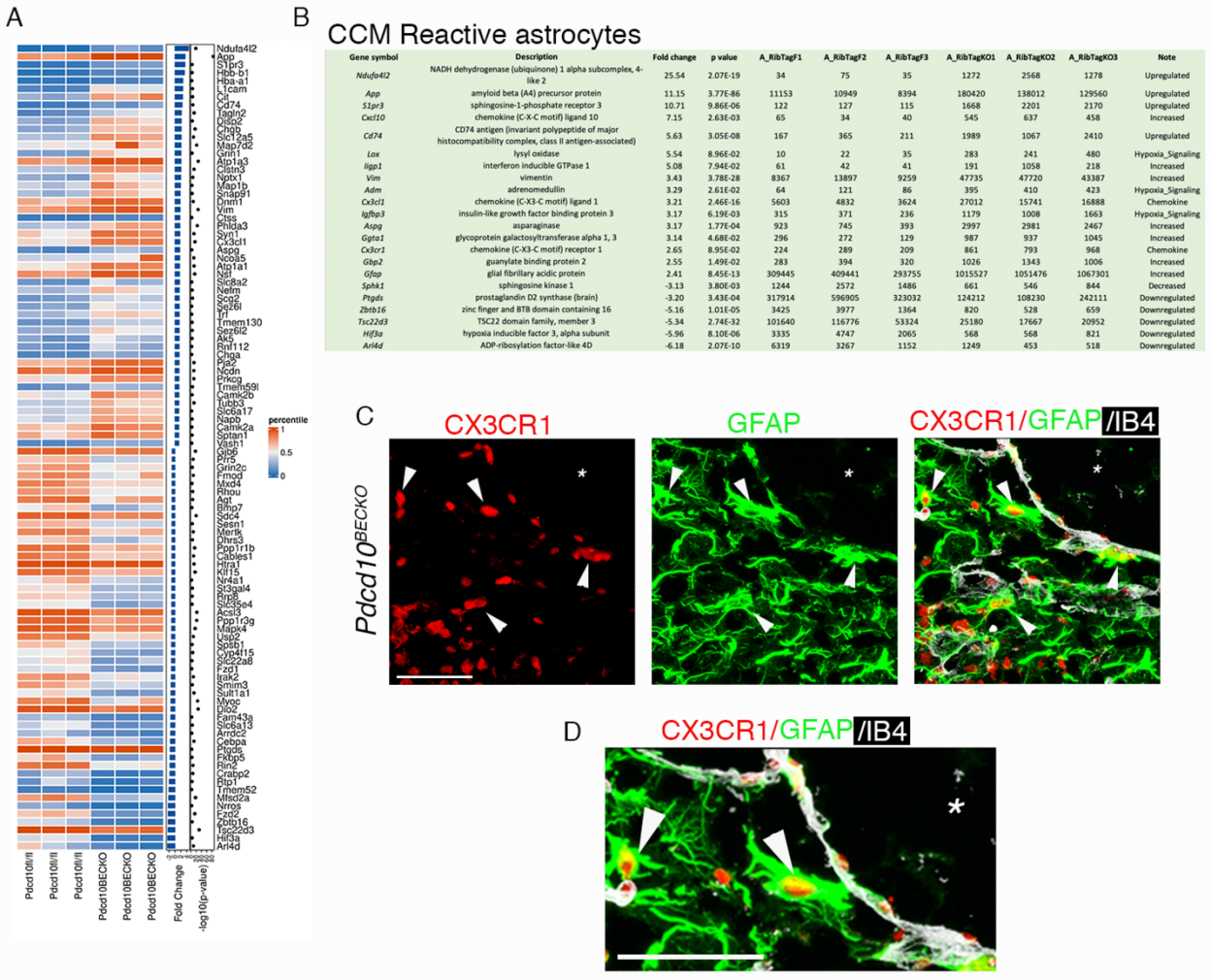

Gene symbol	Description	Fold change	p value	A_RibTagF1	A_RibTagF2	A_RibTagF3	A_RibTagKO1	A_RibTagKO2	A_RibTagKO3	Note
Ndufa4l2	NADH dehydrogenase (ubiquinone) 1 alpha subcomplex, 4-like 2	25.54	2.07E-19	34	75	35	1272	2568	1278	Upregulated
App	amyloid beta (A4) precursor protein	11.15	3.77E-86	11153	10949	8394	180420	138012	129560	Upregulated
S1pr3	sphingosine-1-phosphate receptor 3	10.71	9.86E-06	122	127	115	1668	2201	2170	Upregulated
Cxcl10	chemokine (C-X-C motif) ligand 10	7.15	2.63E-03	65	34	40	545	637	458	Increased
Cd74	CD74 antigen (invariant polypeptide of major histocompatibility complex, class II antigen-associated)	5.63	3.05E-08	167	365	211	1989	1067	2410	Upregulated
Lox	lysyl oxidase	5.54	8.96E-02	10	22	35	283	241	480	Hypoxia_Signaling
Iigp1	interferon inducible GTPase 1	5.08	7.94E-02	61	42	41	191	1058	218	Increased
Vim	vimentin	3.43	3.78E-28	8367	13897	9259	47735	47720	43387	Increased
Adm	adrenomedullin	3.29	2.61E-02	64	121	86	395	410	423	Hypoxia_Signaling
Cx3cl1	chemokine (C-X3-C motif) ligand 1	3.21	2.46E-16	5603	4832	3624	27012	15741	16888	Chemokine
Igfbp3	insulin-like growth factor binding protein 3	3.17	6.19E-03	315	371	236	1179	1008	1663	Hypoxia_Signaling
Aspg	asparaginase	3.17	1.77E-04	923	745	393	2997	2981	2467	Increased
Ggta1	glycoprotein galactosyltransferase alpha 1, 3	3.14	4.68E-02	296	272	129	987	937	1045	Increased
Cx3cr1	chemokine (C-X3-C motif) receptor 1	2.65	8.95E-02	224	289	209	861	793	968	Chemokine
Gbp2	guanylate binding protein 2	2.55	1.49E-02	283	394	320	1026	1343	1006	Increased
Gfap	glial fibrillary acidic protein	2.41	8.45E-13	309445	409441	293755	1015527	1051476	1067301	Increased
Sphk1	sphingosine kinase 1	-3.13	3.80E-03	1244	2572	1486	661	546	844	Decreased
Ptgds	prostaglandin D2 synthase (brain)	-3.20	3.43E-04	317914	596905	323032	124212	108230	242111	Downregulated
Zbtb16	zinc finger and BTB domain containing 16	-5.16	1.01E-05	3425	3977	1364	820	528	659	Downregulated
Tsc22d3	TSC22 domain family, member 3	-5.34	2.74E-32	101640	116776	53324	25180	17667	20952	Downregulated
Hif3a	hypoxia inducible factor 3, alpha subunit	-5.96	8.10E-06	3335	4747	2065	568	568	821	Downregulated
Arl4d	ADP-ribosylation factor-like 4D	-6.18	2.07E-10	6319	3267	1152	1249	453	518	Downregulated

Supplemental Figure 3. CCM reactive astrocytes in CCM disease. A, Heatmap where values are normalized by a percentile ranking (percent of values that have an equal or lesser value to each record[62]) of differentially expressed transcripts in P75 *Pdcd10^{BECKO};Aldh1l1-EGFP/Rpl10a* versus littermate control *Pdcd10$^{fl/fl}$;Aldh1l1-EGFP/Rpl10a.* Transcripts are represented on fold change. The significantly down- and up-regulated genes are labeled in red. n = 3 mice in each group. **B,** Gene expression pattern associated with CCM reactive astrocyte from *Pdcd10^{BECKO};Aldh1l1-EGFP/Rpl10a* brains. Fold change and *P* values are shown for each gene. n = 3 mice in each group. **C,** Confocal microscopy of brain from P50 *Pdcd10^{BECKO}* mice stained for CX3CR1 (red), GFAP-positive astrocytes (green) and endothelial marker isolectin B4 (white). Asterisk indicates vascular lumen of CCM lesion. **D,** Magnified region from *C.* Arrowheads indicate colocalization between GFAP+ Astrocytes and CX3CR1 protein. Fold change and *P* values are shown for each gene and reads values for each biological replicate. n = 3 mice in each group.

276

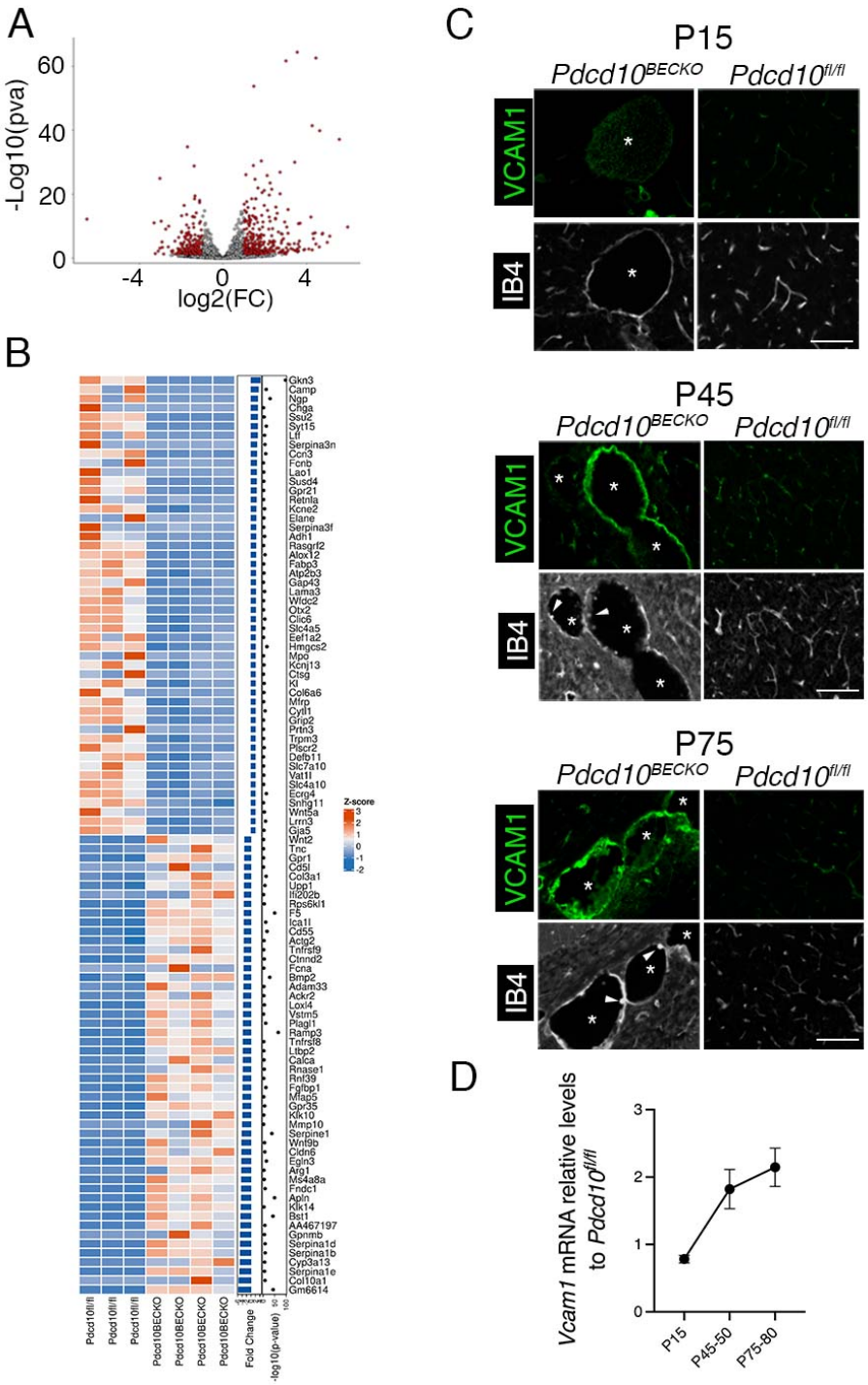

277

278 **Supplemental Figure 4. Inflammation pathway is increased in the CCM endothelium. A,**
279 Volcano plot of differentially expressed transcripts in fresh isolated brain endothelial cells from
280 P75 *Pdcd10^{BECKO};Aldh1l1-EGFP/Rpl10a* versus isolated brain endothelial cells from littermate
281 control *Pdcd10$^{fl/fl}$;Aldh1l1-EGFP/Rpl10a.* Transcripts are represented on a log2 scale from *Fig.*
282 *3A.* **B,** List of the top 50 up- or down-regulated genes from isolated brain endothelial cells obtained

from *Pdcd10*^{BECKO}*;Aldh1l1-EGFP/Rpl10a* brains. Fold change and *P* values are shown for each gene. *Pdcd10*^{BECKO}*;Aldh1l1-EGFP/Rpl10a* mice, n=4; *Pdcd10*$^{fl/fl}$*;Aldh1l1-EGFP/Rpl10a* mice, n=3. Heatmaps comparing the mean expression of DEG. **C,** Immunofluorescence staining of VCAM1 (green) and endothelial marker isolectin B4 (white). Asterisks indicate vascular lumen of CCM lesions of *Pdcd10*^{BECKO} mice at acute (P15), progression (P50), and chronic stage (P80). Arrowhead indicate leukocyte adhered to the endothelial wall in CCM lesions. Fold change and *P* values are shown for each gene. n = 3 mice in each group. **D,** Analysis of *Vcam1* mRNA levels by RT-qPCR in cerebral tissue from mice at acute, progression, and chronic stage as indicated. Data are mean ±SEM, P50 mice n = 4; P15 and P80 mice n = 6.

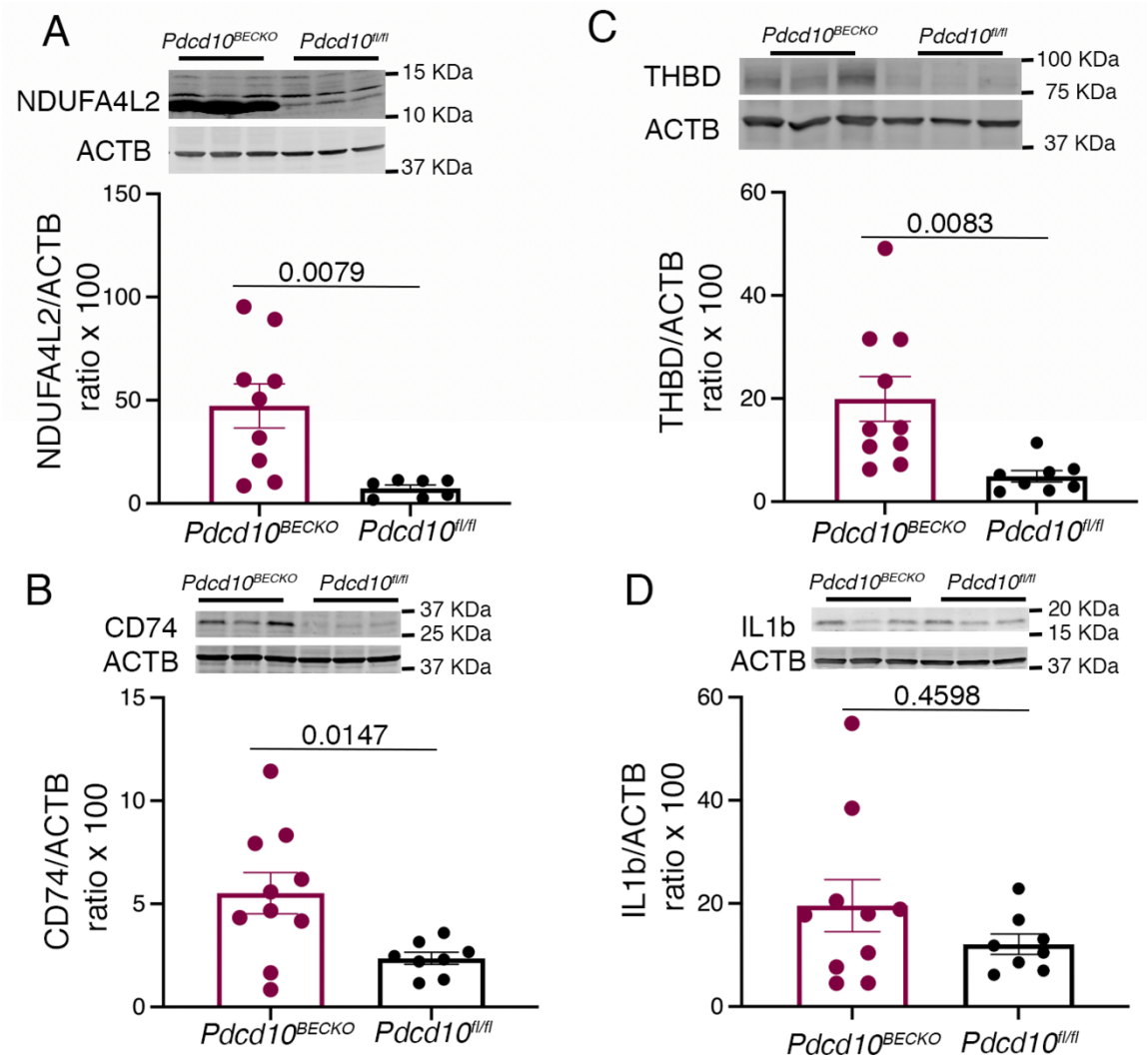

Supplemental Figure 5. Validation of CCM endothelium and reactive astrocyte proteins increased in the CCM brain tissue. A, Quantification of NDUFA4L2 protein in P80 *Pdcd10*^{BECKO} brains compared to *Pdcd10*$^{fl/fl}$ brain controls by western blot. Data are mean ±SEM, *Pdcd10*^{BECKO} mice, n=9; *Pdcd10*$^{fl/fl}$ mice, n=7 (2-tailed Mann-Whitney test). **B,** Quantification of CD74 protein in P80 *Pdcd10*^{BECKO} brains compared to *Pdcd10*$^{fl/fl}$ brain controls by western blot. Data are mean ±SEM, *Pdcd10*^{BECKO} mice, n=10; *Pdcd10*$^{fl/fl}$ mice, n=8 (2-tailed unpaired *t* test). **C,** Quantification of THBD (TM) protein in P80 *Pdcd10*^{BECKO} brains compared to *Pdcd10*$^{fl/fl}$ brain controls by western

blot. Data are mean ±SEM, *Pdcd10*^{BECKO} mice, n=10; *Pdcd10*$^{fl/fl}$ mice, n=8 (2-tailed unpaired *t* test). **D,** Quantification of IL1b protein in P80 *Pdcd10*^{BECKO} brains compared to *Pdcd10*$^{fl/fl}$ brain controls by Western blot. Data are mean ±SEM, *Pdcd10*^{BECKO} mice, n=10; *Pdcd10*$^{fl/fl}$ mice, n=8 (2-tailed Mann-Whitney test).

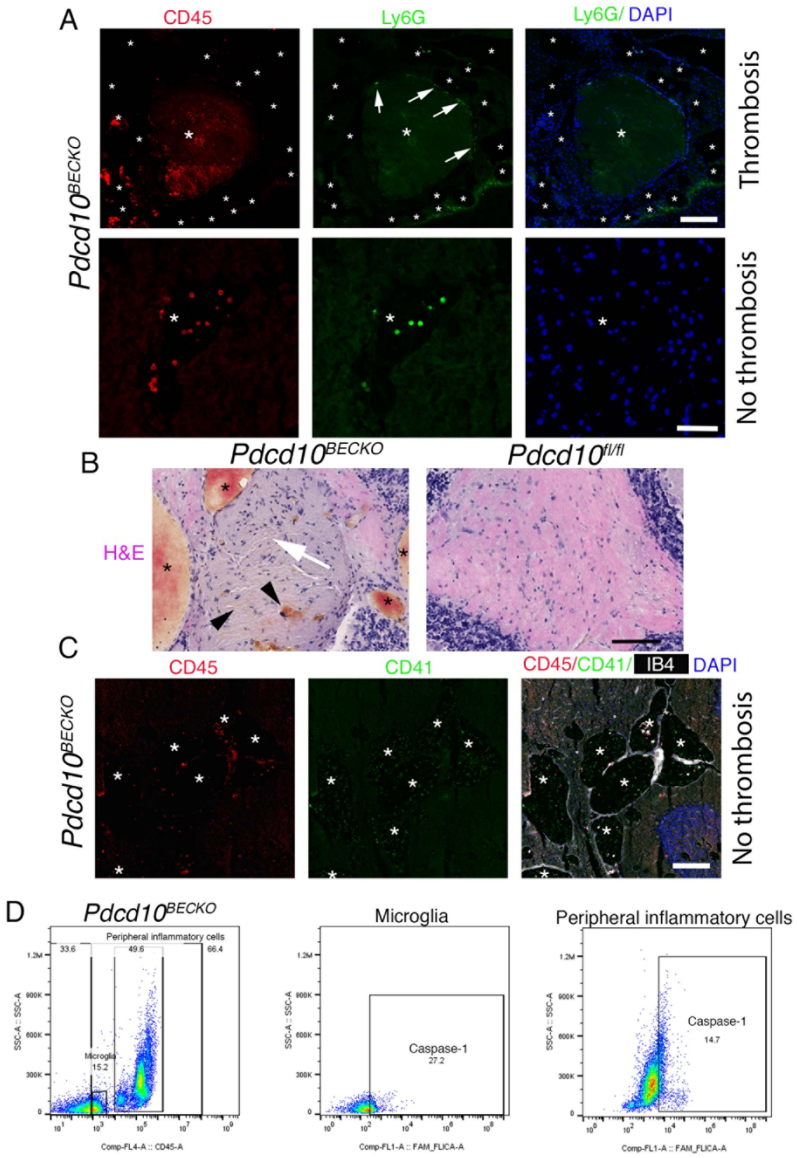

Supplemental Figure 6. Increased presence of CD45+ and Ly6G+ cells in CCM brain tissue. **A,** Immunofluorescence analysis from a serial section used in Fig. 5b and 5c shows leukocyte recruitment CD45+ (red) and accumulation of Ly6G+ neutrophils (green, arrows) in the vascular lumen and vessel wall of lesions in P75 *Pdcd10*^{BECKO} brains, respectively. Non-thrombus lesions also show the presence of Ly6G+ neutrophils (green). Nuclei are labelled by DAPI (blue). Asterisks denote vascular lumen of CCM lesions. Scale bar, 200 μm (top) and 50 μm (bottom). **B,** Hematoxylin & eosin staining of a serial section in Fig. 5g, Arrow indicates an area of thrombosis, arrowheads indicate bleeding, and asterisks denote the vascular lumen of CCM lesions. Scale bar is 100 μm. **C,** Immunofluorescence analysis for leukocytes CD45+ (red), platelets CD41+ (green) cells and labeling of the brain vasculature, using isolectin B4 (white), of

non-thrombotic multi-cavernous lesion in *Pdcd10*^{BECKO} brains. Asterisks denote vascular lumen of CCM lesions. Scale bar, 100 μm. **D,** FACS analysis and quantification of caspase-1 activation in peripheral inflammatory cells (CD45+ high) and microglia (CD45+ low). Data is one experiment representative of 3.

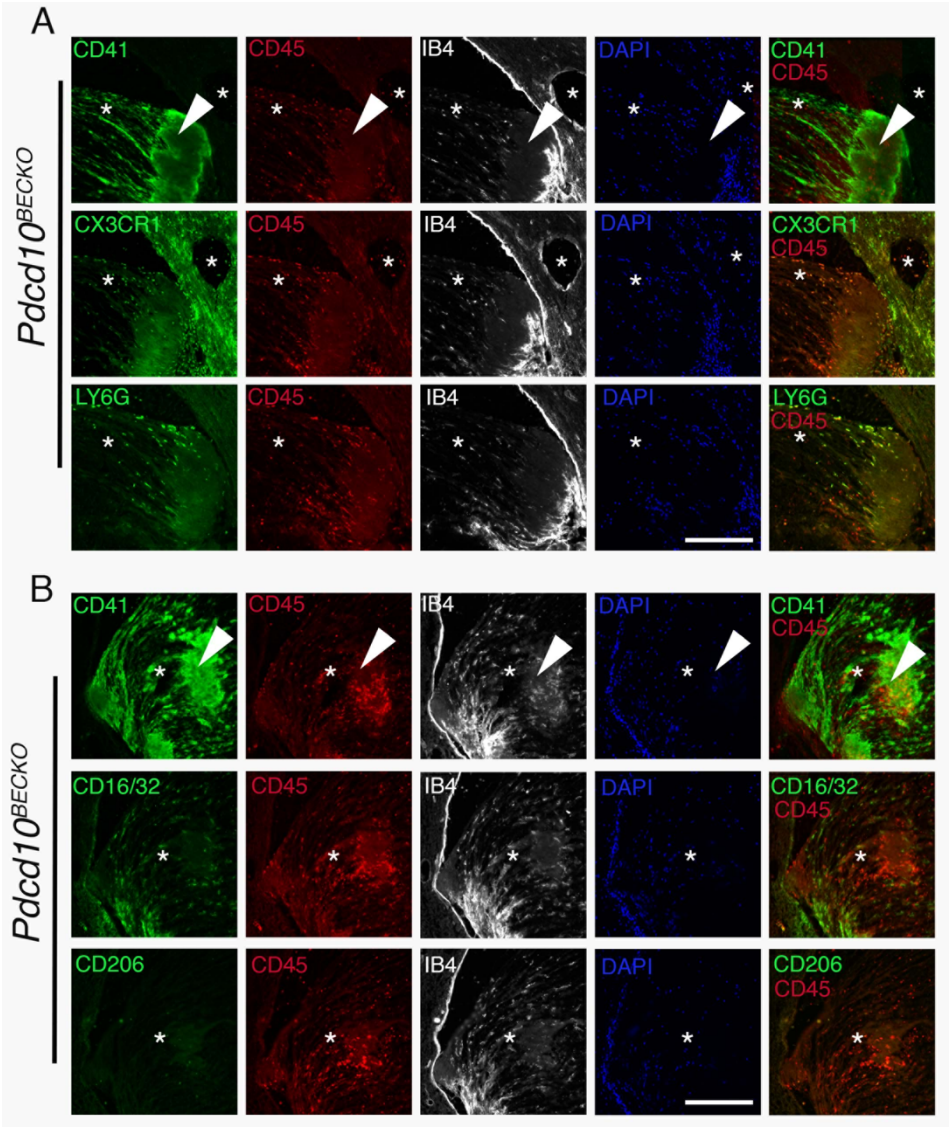

Supplemental Figure 7. Presence of CD45+, CX3CR1+, Ly6G+, and CD16/32+ cells in the thrombosis area of CCM brain tissue. A, Immunofluorescence analysis from serial sections shows leukocyte recruitment CD45+ (red) and accumulation of CX3CR1+ monocytes, Ly6G+ neutrophils in the thrombus (CD41+, green) formed in the vascular lumen of lesions in P75 *Pdcd10*^{BECKO} brains. Asterisks denote vascular lumen of CCM lesions. Arrowheads denote vascular thrombus. Scale bar, 200 μm. Nuclei are labeled by DAPI (blue). **B,** Immunofluorescence analysis from serial sections shows leukocyte recruitment CD45+ (red) and accumulation of CD16/32+ monocytes, but not CD206+ monocytes in the thrombus (CD41+, green) formed in the vascular lumen of a lesion in P75 *Pdcd10*^{BECKO} brains. Asterisks denote vascular lumen of CCM

lesions. Arrowheads denote vascular thrombus. Scale bar, 200 μm. Nuclei are labeled by DAPI (blue).

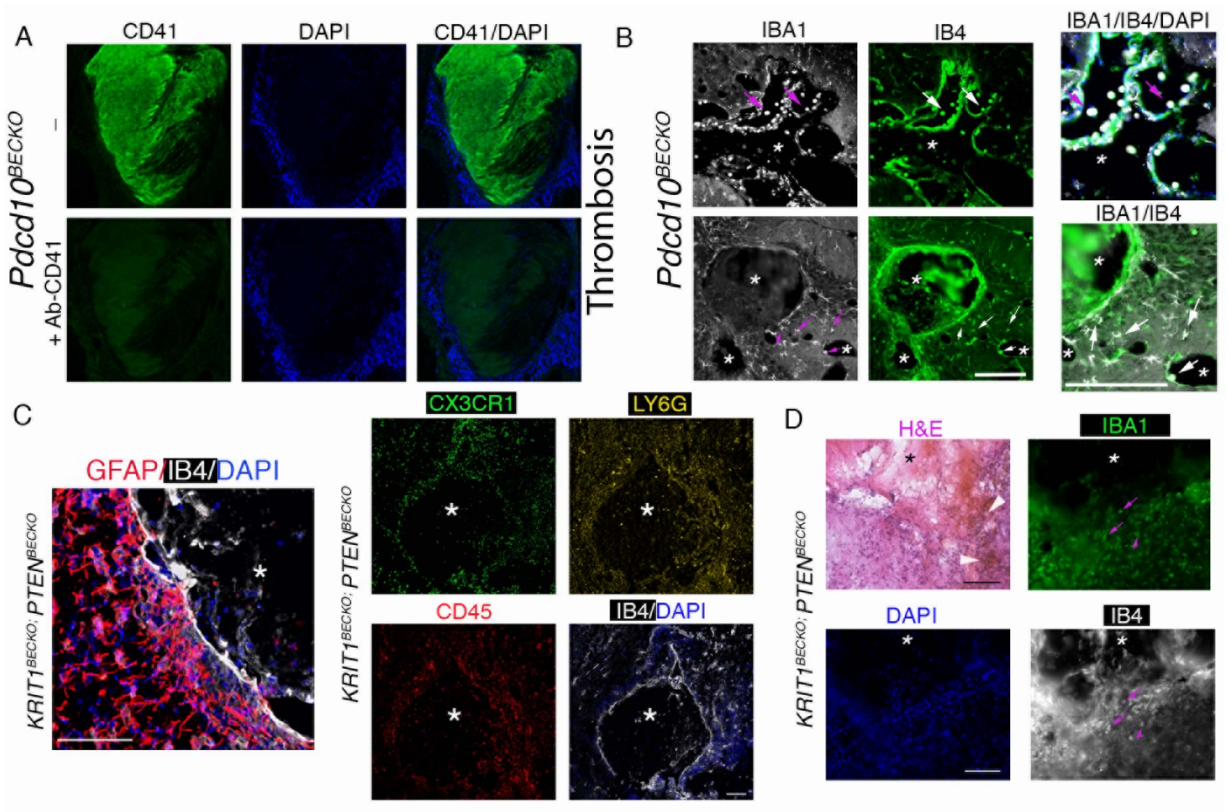

Supplemental Figure 8. Immunofluorescence of CD41+ thrombus and IBA1+IB4 leukocytes in the vascular lumen and brain parenchyma of CCM brain tissue. A, Immunofluorescence analysis of a thrombus (CD41+, green) formed in the vascular lumen of a lesion in P80 *Pdcd10*^{BECKO} brain. To confirm CD41+ immunoreactivity, a serial section was pre-treated with a monoclonal anti-CD41 antibody non-labeled (MWReg30) or vehicle for 1 h at room temperature. After washes, the brain tissue was incubated with a CD41-Alexa-488 antibody (MWReg30). Asterisks denote vascular lumen of CCM lesions. Nuclei are labeled by DAPI (blue). Scale bar, 200 μm. **B,** Immunofluorescence staining of IBA1+ microglia and myeloid cells (white), and endothelial marker isolectin B4 (IB4; green) of cerebral sections from P80 *Pdcd10*^{BECKO}. Immunofluorescence analysis shows IBA1+IB4+ leukocytes (Arrows) in the lumen and brain parenchyma in P80 *Pdcd10*^{BECKO} brains. Asterisks denote vascular lumen of CCM lesions. Scale bar, 200 μm. **C,** Immunofluorescence staining of GFAP+ astrocytes (red) and endothelial marker isolectin B4 (IB4; white) from serial sections of CCM lesions, where leukocyte recruitment CD45+ (red) and accumulation of CX3CR1+ (green), and Ly6G+ neutrophils (yellow) formed in the vascular lumen of a lesion in P50 *Krit1*$^{BECKO;}$*PTEN*$^{BECKO/wt}$ brains. **D,** H&E and immunofluorescence analysis from serial sections shows CCM lesions and leukocyte/microglia recruitment IBA1+ (green) formed in the vascular lumen and CNS parenchyma of lesions in P50 *Krit1*$^{BECKO;}$*PTEN* $^{BECKO/wt}$ spinal cords. Endothelial marker is isolectin B4 (IB4; white). Asterisks denote vascular lumen of CCM lesions. Arrowhead (H&E) and arrows (immunostaining) denote leukocytes. Scale bar, 100 μm. Nuclei are labeled by DAPI (blue).

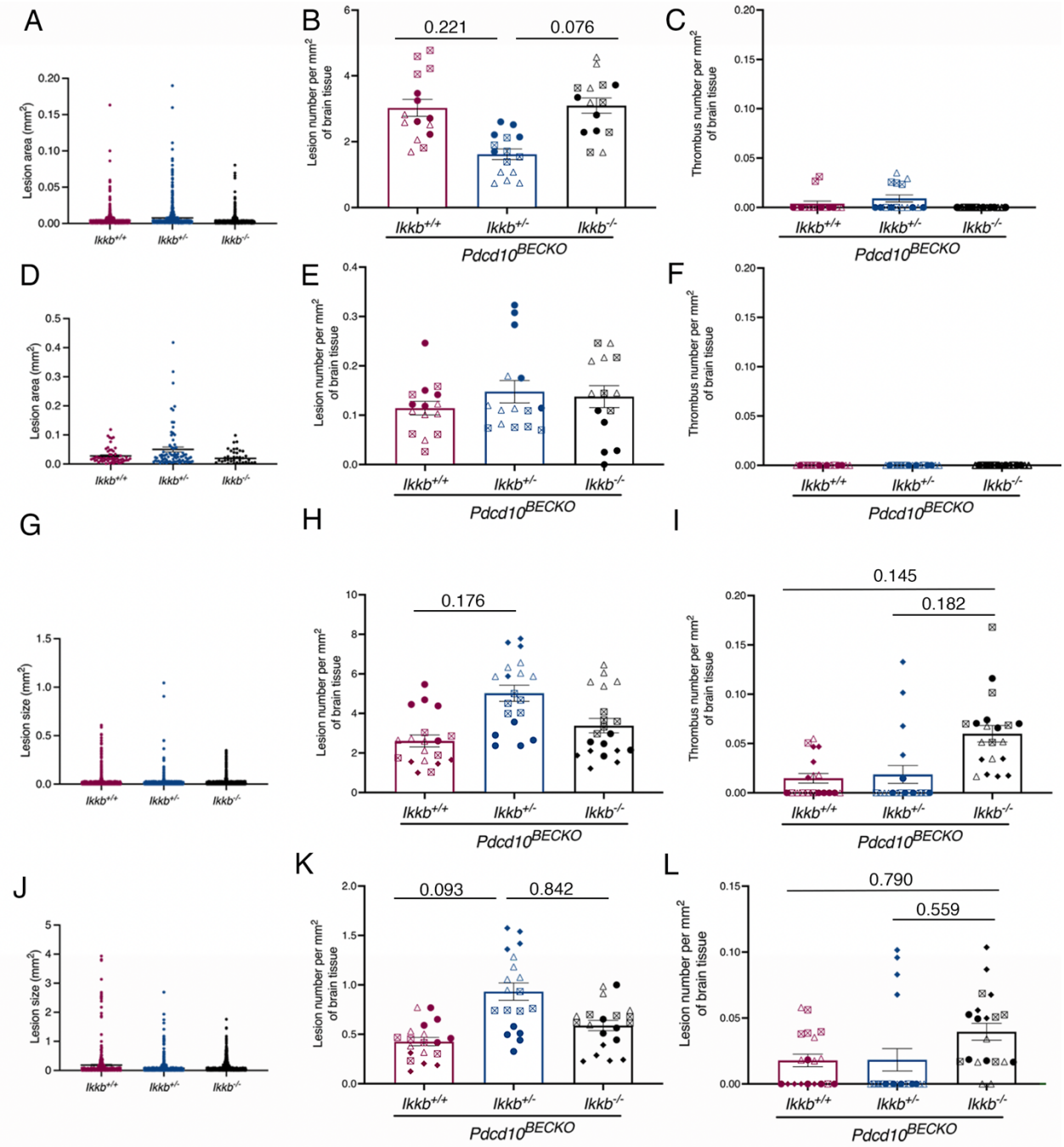

Supplemental Figure 9. Loss of brain endothelial IKKb in acute and progression stage of CCM disease. A, Analysis and quantification of stage 1 (single cavernous) lesion size in P15 *Pdcd10^{BECKO};Ikkb$^{wt/wt}$* (*Pdcd10^{BECKO};Ikkb$^{+/+}$*), *Pdcd10^{BECKO};Ikkb$^{BECKO/wt}$* (*Pdcd10^{BECKO};Ikkb$^{+/-}$*) and *Pdcd10^{BECKO};Ikkb^{BECKO}* (*Pdcd10^{BECKO};Ikkb$^{-/-}$*) brains. **B,** Analysis and quantification of the number of stage 1 lesions per mm² in P15 *Pdcd10^{BECKO};Ikkb $^{wt/ wt}$*, *Pdcd10^{BECKO};Ikkb$^{BECKO/wt}$* and *Pdcd10^{BECKO};Ikkb^{BECKO}* brains. **C,** Analysis and quantification of the number of thrombi in stage 1 lesions per mm² in P15 *Pdcd10^{BECKO};Ikkb $^{wt/ wt}$*, *Pdcd10^{BECKO};Ikkb$^{BECKO/wt}$* and *Pdcd10^{BECKO};Ikkb^{BECKO}* brains. **D,** Analysis and quantification of stage 2 (multi-cavernous) lesion size in P15 *Pdcd10^{BECKO};Ikkb$^{wt/wt}$*, *Pdcd10^{BECKO};Ikkb$^{BECKO/wt}$* and *Pdcd10^{BECKO};Ikkb^{BECKO}* brains. **E,**

Analysis and quantification of the number of stage 2 lesions per mm² in P15 *Pdcd10^{BECKO}; Ikkb$^{wt/wt}$*, *Pdcd10^{BECKO};Ikkb$^{BECKO/wt}$* and *Pdcd10^{BECKO};Ikkb^{BECKO}* brains. **F,** Analysis and quantification of the number of thrombi in stage 2 lesions per mm² in P15 *Pdcd10^{BECKO}; Ikkb$^{wt/wt}$*, *Pdcd10^{BECKO};Ikkb$^{BECKO/wt}$* and *Pdcd10^{BECKO};Ikkb^{BECKO}* brains. **G,** Analysis and quantification of stage 1 (single cavernous) lesion size in P50 *Pdcd10^{BECKO}; Ikkb$^{wt/wt}$*, *Pdcd10^{BECKO};Ikkb$^{BECKO/wt}$* and *Pdcd10^{BECKO};Ikkb^{BECKO}* brains. **H,** Analysis and quantification of the number of stage 1 lesions per mm² in P50 *Pdcd10^{BECKO}; Ikkb$^{wt/wt}$*, *Pdcd10^{BECKO};Ikkb$^{BECKO/wt}$* and *Pdcd10^{BECKO};Ikkb^{BECKO}* brains. **I,** Analysis and quantification of the number of thrombi in stage 1 lesions per mm² in P50 *Pdcd10^{BECKO};I Ikkb$^{wt/wt}$*, *Pdcd10^{BECKO};Ikkb$^{BECKO/wt}$* and *Pdcd10^{BECKO};Ikkb^{BECKO}* brains. **J,** Analysis and quantification of stage 2 (multi-cavernous) lesion size in P50 *Pdcd10^{BECKO}; Ikkb$^{wt/wt}$*, *Pdcd10^{BECKO};Ikkb$^{BECKO/wt}$* and *Pdcd10^{BECKO};Ikkb^{BECKO}* brains. **K,** Analysis and quantification of the number of stage 2 lesions per mm² in P50 *Pdcd10^{BECKO};Ikkb$^{wt/wt}$*, *Pdcd10^{BECKO};Ikkb$^{BECKO/wt}$* and *Pdcd10^{BECKO};Ikkb^{BECKO}* brains. **L,** Analysis and quantification of the number of thrombi in stage 2 lesions per mm² in P50 *Pdcd10^{BECKO}; Ikkb$^{wt/wt}$*, *Pdcd10^{BECKO};Ikkb$^{BECKO/wt}$* and *Pdcd10^{BECKO};Ikkb^{BECKO}* brains. Animals were injected at P1 with 4-hydroxi-tamoxifen. Statistical analysis is based on the average of 5 sections per animal. Data regarding lesion number per area and thrombosis from each individual section is represented by three (B, C, E, F) or four (H, I, K, L) different symbol shapes in the graphs, each set of shapes represents one animal *(*per group: *filled circle,* animal 1; *triangle,* animal 2; *square,* animal 3; *rhomboid,* animal 4). All data are mean ±SEM. P15 mice, n=3; P50 mice, n=4 (Kruskal-Wallis post hoc Dunn's test).

Data Supplement Statistical Table

Online Statistical Analysis Data Tables

Online table I: Sample size and normality test for data presented in main figures.

Figure	Sample Group	Sample size	Shapiro-Wilk normality test P value	Passed normality test
Figure 4B	PDCD10^{BECKO}	3	0.7838	Yes
	PDCD10^{BECKO} + MCC950	3	0.2142	Yes
	PDCD10$^{fl/fl}$	3	0.4489	Yes
Figure 4D	PDCD10^{BECKO}	10	0.4297	Yes
	PDCD10$^{fl/fl}$	8	0.5691	Yes
Figure 5D	PDCD10^{BECKO}	5	N too small	N/A
	PDCD10$^{fl/fl}$	6	0.3253	Yes
Figure 5E	PDCD10^{BECKO} Neut	5	N too small	N/A
	PDCD10$^{fl/fl}$ Neut	6	0.0044	No
	PDCD10^{BECKO} Micro	5	N too small	No
	PDCD10$^{fl/fl}$ Micro	6	0.2742	Yes
	PDCD10^{BECKO} C mono	5	N too small	No
	PDCD10$^{fl/fl}$ C mono	6	0.3633	Yes

	$PDCD10^{BECKO}$ NC mono $PDCD10^{fl/fl}$ NC mono $PDCD10^{BECKO}$ DC $PDCD10^{fl/fl}$ DC	5 6 5 5	N too small 0.9628 N too small N too small	No Yes N/A N/A
Figure 5F	$PDCD10^{BECKO}$ CD4 $PDCD10^{fl/fl}$ CD4 $PDCD10^{BECKO}$ CD8 $PDCD10^{fl/fl}$ CD8 $PDCD10^{BECKO}$ B cells $PDCD10^{fl/fl}$ B cells	5 6 5 6 5 6	N too small 0.1930 N too small 0.0179 N too small 0.0259	N/A N/A N/A No N/A No
Figure 5J	$PDCD10^{BECKO}$ $PDCD10^{fl/fl}$	3 3	0.7235 0.4821	Yes Yes
Figure 6A-E, G	$PDCD10^{BECKO}$;$Ikkb^{+/+}$ $PDCD10^{BECKO}$;$Ikkb^{+/-}$ $PDCD10^{BECKO}$;$Ikkb^{-/-}$	3 3 3	N too small N too small N too small	N/A N/A N/A

392 **Online table II: Statistical tests and P values for data presented in main figures.**

Figure	Statistical test	Sample Group	P value
Figure 4B	One-Way ANOVA followed by Tukey's multiple comparisons test	$PDCD10^{BECKO}$ vs $PDCD10^{BECKO}$ + MCC950 $PDCD10^{BECKO}$ vs $PDCD10^{fl/fl}$ $PDCD10^{BECKO}$ + MCC950 vs $PDCD10^{fl/fl}$	0.001 $1.192x10^{-4}$ 0.034
Figure 4D	Unpaired two-tailed *t* test	$PDCD10^{BECKO}$ vs $PDCD10^{fl/fl}$	0.0017
Figure 5D	Two-tailed Mann-Whitney test	$PDCD10^{BECKO}$ vs $PDCD10^{fl/fl}$	0.0043
Figure 5E	Two-tailed Mann-Whitney test Two-tailed Mann-Whitney test Two-tailed Mann-Whitney test Two-tailed Mann-Whitney test Two-tailed Mann-Whitney test	$PDCD10^{BECKO}$ vs $PDCD10^{fl/fl}$ Neut $PDCD10^{BECKO}$ vs $PDCD10^{fl/fl}$ Micro $PDCD10^{BECKO}$ vs $PDCD10^{fl/fl}$ C Mono $PDCD10^{BECKO}$ vs $PDCD10^{fl/fl}$ NC Mono $PDCD10^{BECKO}$ vs $PDCD10^{fl/fl}$ DC	0.0043 0.0043 0.0043 0.0043 0.0043

Figure 5F	Two-tailed Mann-Whitney test Two-tailed Mann-Whitney test Two-tailed Mann-Whitney test	$PDCD10^{BECKO}$ vs $PDCD10^{fl/fl}$ CD4 $PDCD10^{BECKO}$ vs $PDCD10^{fl/fl}$ CD8 $PDCD10^{BECKO}$ vs $PDCD10^{fl/fl}$ B cells	0.0303 0.0043 0.0043
Figure 5J	Unpaired two-tailed *t* test	$PDCD10^{BECKO}$ vs $PDCD10^{fl/fl}$	0.0012
Figure 6A	Kruskal-Wallis test followed by Dunn's multiple comparisons test	$PDCD10^{BECKO}$;$Ikkb^{+/+}$ vs $PDCD10^{BECKO}$;$Ikkb^{+/-}$ $PDCD10^{BECKO}$;$Ikkb^{+/+}$ vs $PDCD10^{BECKO}$;$Ikkb^{-/-}$ $PDCD10^{BECKO}$;$Ikkb^{+/-}$ vs $PDCD10^{BECKO}$;$Ikkb^{-/-}$	0.303 0.051 >0.999
Figure 6B	Kruskal-Wallis test followed by Dunn's multiple comparisons test	$PDCD10^{BECKO}$;$Ikkb^{+/+}$ vs $PDCD10^{BECKO}$;$Ikkb^{+/-}$ $PDCD10^{BECKO}$;$Ikkb^{+/+}$ vs $PDCD10^{BECKO}$;$Ikkb^{-/-}$ $PDCD10^{BECKO}$;$Ikkb^{+/-}$ vs $PDCD10^{BECKO}$;$Ikkb^{-/-}$	0.324 0.045 0.325
Figure 6C	Kruskal-Wallis test followed by Dunn's multiple comparisons test	$PDCD10^{BECKO}$;$Ikkb^{+/+}$ vs $PDCD10^{BECKO}$;$Ikkb^{+/-}$ $PDCD10^{BECKO}$;$Ikkb^{+/+}$ vs $PDCD10^{BECKO}$;$Ikkb^{-/-}$ $PDCD10^{BECKO}$;$Ikkb^{+/-}$ vs $PDCD10^{BECKO}$;$Ikkb^{-/-}$	0.095 0.091 >0.999
Figure 6D	Kruskal-Wallis test followed by Dunn's multiple comparisons test	$PDCD10^{BECKO}$;$Ikkb^{+/+}$ vs $PDCD10^{BECKO}$;$Ikkb^{+/-}$ $PDCD10^{BECKO}$;$Ikkb^{+/+}$ vs $PDCD10^{BECKO}$;$Ikkb^{-/-}$ $PDCD10^{BECKO}$;$Ikkb^{+/-}$ vs $PDCD10^{BECKO}$;$Ikkb^{-/-}$	>0.999 0.076 0.539
Figure 6E	Kruskal-Wallis test followed by Dunn's multiple comparisons test	$PDCD10^{BECKO}$;$Ikkb^{+/+}$ vs $PDCD10^{BECKO}$;$Ikkb^{+/-}$	0.915

		PDCD10^{BECKO};Ikkb$^{+/+}$ vs PDCD10^{BECKO};Ikkb$^{-/-}$	0.542
		PDCD10^{BECKO};Ikkb$^{+/-}$ vs PDCD10^{BECKO};Ikkb$^{-/-}$	0.769
Figure 6G	Kruskal-Wallis test followed by Dunn's multiple comparisons test	PDCD10^{BECKO};Ikkb$^{+/+}$ vs PDCD10^{BECKO};Ikkb$^{+/-}$	0.303
		PDCD10^{BECKO};Ikkb$^{+/+}$ vs PDCD10^{BECKO};Ikkb$^{-/-}$	0.890
		PDCD10^{BECKO};Ikkb$^{+/-}$ vs PDCD10^{BECKO};Ikkb$^{-/-}$	>0.999

Online table III: Sample size and normality test for data presented in supplemental figures.

Figure	Sample Group	Sample size	Shapiro-Wilk normality test P value	Passed normality test
Supp. Figure 5A	PDCD10^{BECKO} PDCD10$^{fl/fl}$	9 7	0.4374 0.0479	Yes No
Supp. Figure 5B	PDCD10^{BECKO} PDCD10$^{fl/fl}$	10 8	0.8987 0.7719	Yes Yes
Supp. Figure 5C	PDCD10^{BECKO} PDCD10$^{fl/fl}$	10 8	0.1014 0.1415	Yes Yes
Supp. Figure 5D	PDCD10^{BECKO} PDCD10$^{fl/fl}$	10 8	0.0436 0.4254	No Yes
Supp. Figure 9A-L	PDCD10^{BECKO};Ikkb$^{+/+}$ PDCD10^{BECKO};Ikkb$^{+/-}$ PDCD10^{BECKO};Ikkb$^{-/-}$	3 3 3	N too small N too small N too small	N/A N/A N/A

Online table IV: Statistical tests and P values for data presented in supplemental figures.

Figure	Statistical test	Sample Group	P value
Supp. Figure 5A	Two-tailed Mann-Whitney test	PDCD10^{BECKO} vs PDCD10$^{fl/fl}$	0.0079
Supp. Figure 5B	Unpaired two-tailed *t* test	PDCD10^{BECKO} vs PDCD10$^{fl/fl}$	0.0147
Supp. Figure 5C	Unpaired two-tailed *t* test	PDCD10^{BECKO} vs PDCD10$^{fl/fl}$	0.0083

Supp. Figure 5D	Two-tailed Mann-Whitney test	$PDCD10^{BECKO}$ vs $PDCD10^{fl/fl}$	0.4598
Supp. Figure 9A	Kruskal-Wallis test followed by Dunn's multiple comparisons test	$PDCD10^{BECKO}$;$Ikkb^{+/+}$ vs $PDCD10^{BECKO}$;$Ikkb^{+/-}$ $PDCD10^{BECKO}$;$Ikkb^{+/+}$ vs $PDCD10^{BECKO}$;$Ikkb^{-/-}$ $PDCD10^{BECKO}$;$Ikkb^{+/-}$ vs $PDCD10^{BECKO}$;$Ikkb^{-/-}$	0.121 0.863 0.062
Supp. Figure 9B	Kruskal-Wallis test followed by Dunn's multiple comparisons test	$PDCD10^{BECKO}$;$Ikkb^{+/+}$ vs $PDCD10^{BECKO}$;$Ikkb^{+/-}$ $PDCD10^{BECKO}$;$Ikkb^{+/+}$ vs $PDCD10^{BECKO}$;$Ikkb^{-/-}$ $PDCD10^{BECKO}$;$Ikkb^{+/-}$ vs $PDCD10^{BECKO}$;$Ikkb^{-/-}$	0.221 >0.999 0.076
Supp. Figure 9C	Kruskal-Wallis test followed by Dunn's multiple comparisons test	$PDCD10^{BECKO}$;$Ikkb^{+/+}$ vs $PDCD10^{BECKO}$;$Ikkb^{+/-}$ $PDCD10^{BECKO}$;$Ikkb^{+/+}$ vs $PDCD10^{BECKO}$;$Ikkb^{-/-}$ $PDCD10^{BECKO}$;$Ikkb^{+/-}$ vs $PDCD10^{BECKO}$;$Ikkb^{-/-}$	0.749 >0.999 0.230
Supp. Figure 9D	Kruskal-Wallis test followed by Dunn's multiple comparisons test	$PDCD10^{BECKO}$;$Ikkb^{+/+}$ vs $PDCD10^{BECKO}$;$Ikkb^{+/-}$ $PDCD10^{BECKO}$;$Ikkb^{+/+}$ vs $PDCD10^{BECKO}$;$Ikkb^{-/-}$ $PDCD10^{BECKO}$;$Ikkb^{+/-}$ vs $PDCD10^{BECKO}$;$Ikkb^{-/-}$	0.470 0.994 0.418
Supp. Figure 9E	Kruskal-Wallis test followed by Dunn's multiple comparisons test	$PDCD10^{BECKO}$;$Ikkb^{+/+}$ vs $PDCD10^{BECKO}$;$Ikkb^{+/-}$ $PDCD10^{BECKO}$;$Ikkb^{+/+}$ vs $PDCD10^{BECKO}$;$Ikkb^{-/-}$ $PDCD10^{BECKO}$;$Ikkb^{+/-}$ vs $PDCD10^{BECKO}$;$Ikkb^{-/-}$	0.830 0.880 0.991

Supp. Figure 9F	Kruskal-Wallis test followed by Dunn's multiple comparisons test	$PDCD10^{BECKO}$;$Ikkb^{+/+}$ vs $PDCD10^{BECKO}$;$Ikkb^{+/-}$ $PDCD10^{BECKO}$;$Ikkb^{+/+}$ vs $PDCD10^{BECKO}$;$Ikkb^{-/-}$ $PDCD10^{BECKO}$;$Ikkb^{+/-}$ vs $PDCD10^{BECKO}$;$Ikkb^{-/-}$	ns ns ns
Supp. Figure 9G	Kruskal-Wallis test followed by Dunn's multiple comparisons test	$PDCD10^{BECKO}$;$Ikkb^{+/+}$ vs $PDCD10^{BECKO}$;$Ikkb^{+/-}$ $PDCD10^{BECKO}$;$Ikkb^{+/+}$ vs $PDCD10^{BECKO}$;$Ikkb^{-/-}$ $PDCD10^{BECKO}$;$Ikkb^{+/-}$ vs $PDCD10^{BECKO}$;$Ikkb^{-/-}$	0.187 0.464 0.775
Supp. Figure 9H	Kruskal-Wallis test followed by Dunn's multiple comparisons test	$PDCD10^{BECKO}$;$Ikkb^{+/+}$ vs $PDCD10^{BECKO}$;$Ikkb^{+/-}$ $PDCD10^{BECKO}$;$Ikkb^{+/+}$ vs $PDCD10^{BECKO}$;$Ikkb^{-/-}$ $PDCD10^{BECKO}$;$Ikkb^{+/-}$ vs $PDCD10^{BECKO}$;$Ikkb^{-/-}$	0.176 0.822 0.398
Supp. Figure 9I	Kruskal-Wallis test followed by Dunn's multiple comparisons test	$PDCD10^{BECKO}$;$Ikkb^{+/+}$ vs $PDCD10^{BECKO}$;$Ikkb^{+/-}$ $PDCD10^{BECKO}$;$Ikkb^{+/+}$ vs $PDCD10^{BECKO}$;$Ikkb^{-/-}$ $PDCD10^{BECKO}$;$Ikkb^{+/-}$ vs $PDCD10^{BECKO}$;$Ikkb^{-/-}$	>0.999 0.145 0.182
Supp. Figure 9J	Kruskal-Wallis test followed by Dunn's multiple comparisons test	$PDCD10^{BECKO}$;$Ikkb^{+/+}$ vs $PDCD10^{BECKO}$;$Ikkb^{+/-}$ $PDCD10^{BECKO}$;$Ikkb^{+/+}$ vs $PDCD10^{BECKO}$;$Ikkb^{-/-}$ $PDCD10^{BECKO}$;$Ikkb^{+/-}$ vs $PDCD10^{BECKO}$;$Ikkb^{-/-}$	0.191 0.613 0.628

Supp. Figure 9K	Kruskal-Wallis test followed by Dunn's multiple comparisons test	$PDCD10^{BECKO}$;$Ikkb^{+/+}$ vs $PDCD10^{BECKO}$;$Ikkb^{+/-}$	0.093
		$PDCD10^{BECKO}$;$Ikkb^{+/+}$ vs $PDCD10^{BECKO}$;$Ikkb^{-/-}$	0.842
		$PDCD10^{BECKO}$;$Ikkb^{+/-}$ vs $PDCD10^{BECKO}$;$Ikkb^{-/-}$	0.398
Supp. Figure 9L	Kruskal-Wallis test followed by Dunn's multiple comparisons test	$PDCD10^{BECKO}$;$Ikkb^{+/+}$ vs $PDCD10^{BECKO}$;$Ikkb^{+/-}$	>0.999
		$PDCD10^{BECKO}$;$Ikkb^{+/+}$ vs $PDCD10^{BECKO}$;$Ikkb^{-/-}$	0.790
		$PDCD10^{BECKO}$;$Ikkb^{+/-}$ vs $PDCD10^{BECKO}$;$Ikkb^{-/-}$	0.559